BEATS

Workpackage 3
The X Ray source

Report on magnet measurements and characterisation

D 3.6

March 2022

Funded by the EU's H2020 framework programme under grant agreement n°822535

PROJECT DETAILS

PROJECT ACRONYM
BEATS

PROJECT TITLE
BEAmline for Tomography at SESAME

GRANT AGREEMENT NO:
822535

THEME

START DATE
2019

DELIVERABLE DETAILS

WORK PACKAGE ID 03

EXPECTED DATE: 30/06/2021

WORK PACKAGE TITLE: THE X-RAY SOURCE

DELIVERABLE TITLE: REPORT ON MAGNET MEASUREMENTS AND CHARACTERISATION

WORK PACKAGE LEADER: INFN

DELIVERABLE DESCRIPTION: REPORT

DELIVERABLE ID: D3.6

PERSON RESPONSIBLE FOR THE DELIVERABLE
Jordi Marcos Ruzafa (ALBA)

NATURE

☒ R - Report ☐ P - Prototype ☐ D - Demonstrator ☐ O - Other

DISSEMINATION LEVEL

☒ P - Public
☐ PP - Restricted to other programme participants & EC:
☐ RE - Restricted to a group
☐ CO - Confidential, only for members of the consortium

REPORT DETAILS

VERSION: 1

DATE
04/03/2022

NUMBER OF PAGES
13

DELIVERABLE REPORT AUTHOR(S): J.MARCOS

FOR MORE INFO PLEASE CONTACT: JMARCOS@CELLS.ES

STATUS

☐ Template ☒ Draft
☐ Final ☐ Released to the EC

CONTENTS

Introduction **4**
Acceptance criteria 4
Measurement strategy 4
Obtained results **5**
Field maps: field profile, maximum field and roll-off 5
Integrated measurements: field integrals and multipoles 7
Correction coils 10
Compliance with specifications **13**

INTRODUCTION

In this document, we present the results of the magnetic validation and characterization of the 3-pole wiggler (3PW) device that will be used as the x-ray source for the BEATS beamline at SESAME. The device has been manufactured by Kyma Srl, Slowenia. The measurements presented here were carried out at the manufacturer's premises at the end of January 2022.

Acceptance criteria

The magnetic acceptance criteria for the device, as requested in the Technical Specifications of the Call for Tender and subsequently agreed with the manufacturing company, are summarized in Table 1.

Table 1: Acceptance criteria for the magnetic FAT of the 3PW device.

Parameter	Required value
Peak field of central pole	>2.9 Tesla @ 11mm gap
Field roll off at x=5mm	$<2.4\times10^{-5}$
Field roll off at x=10mm	$<1.3\times10^{-4}$
Field roll off at x=20mm	$<5.0\times10^{-3}$
On-axis first field integrals Ix,Iz (no CC)	$<5.0\times10^{-5}$ T·m
On-axis second field integrals I2x,I2z (no CC)	$<5.0\times10^{-5}$ T·m^2
Integrated quadrupole within x=±20mm	$<\|1.0\|\times10^{-2}$ T
Integrated sextupole within x=±20mm	<|1.0| T/m
Integrated octupole within x=±20mm	$<\|1.0\|\times10^{2}$ T/m^2

Measurement strategy

In order to verify the requirements listed in Table 1, a combination of integrated (flipping coil) and local (Hall probe) field measurements was carried out. The set of magnetic measurements included:

1. **2D Field scans with Hall probe:** These field scans were performed at a series of selected gaps between the minimum (11mm) and maximum (300mm) settings, on the magnet midplane. The goal of these measurements was to define the peak field dependence vs gap and the magnetic field roll-off. In particular, they shall allow verifying that a central field larger than 2.9T is obtained at minimum gap (11mm). The horizontal range of the magnetic field scans covered the maximum range specified for the roll off (+/-20mm). The sampling step of the scans was 10μm along the longitudinal direction (fixed by the characteristics of the measurement system) and 5mm along the transversal direction.
2. **Vertical dependence of the magnetic field at the central pole:** This characterization was done by means of Hall probe measurements in order to verify the location of the device's midplane.
3. **Field integral measurements:** These measurements were performed with a flipping coil system, and have been used to validate the on-axis field integrals (first and second) and the

integrated multipoles. Characterization was carried out at the same set of gaps analysed with the Hall probe (point 1, 2D field scans, above) and for the same horizontal range (+/-20mm), with a more detailed sampling step of 1mm.

4. **Characterization of correction coils:** The integrated effect of each one of the 4 correction coils at a given current was measured with the flipping coil system. The correction coils' integrated field signatures have been combined afterwards with the field integral measurements in order to determine a table of correction coil current settings (look-up table) at different gaps. The obtained table will be used to check experimentally the cancellation of the 3PW residual integrated field at least at minimum gap (11 mm).

It was agreed to carry out the full characterization described in points 1 and 3 of the previous list at the following gap settings (in [mm]): 11, 12, 14, 16, 18, 20, 25, 30, 40, 50, 60, 70, 80, 90, 100, 125, 150, 175, and 200. In addition to these measurements, a complementary set of simplified on-axis measurements was also performed for a much larger set of gap values reaching up to maximum gap (300mm)

OBTAINED RESULTS

Field maps: field profile, maximum field and roll-off

The field profile of the device along the longitudinal axis (at X=0) at minimum gap (11mm) is shown in Figure 1, together with the expected profile obtained from RADIA simulations. As can be seen, the experimental profile is very close to the expected one, with a difference smaller than 30mT all over the longitudinal range. In particular, the field value at the centre of the pole is 2.917T, thus satisfying the requirement $(B_z)_{max}$>2.9T.

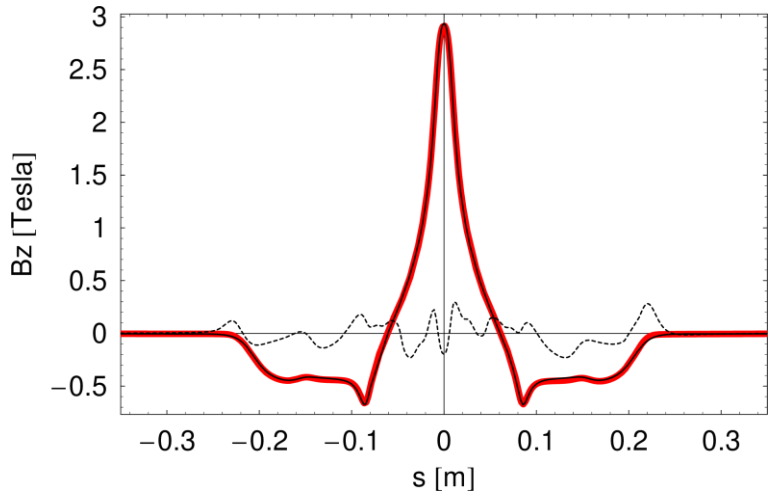

Figure 1: Profile of the vertical component of the magnetic field along the longitudinal axis of the 3PW device, for a gap of 11mm. The thick red corresponds to the experimental data, the solid black line to the theoretical model (RADIA simulation), and the dashed black line stands for the difference between the two curves magnified by a factor 10.

The dependence of the peak field generated by the device to the gap opening is shown in Figure 2. It is interesting to note that the peak field at maximum gap (300mm) is still 64mT.

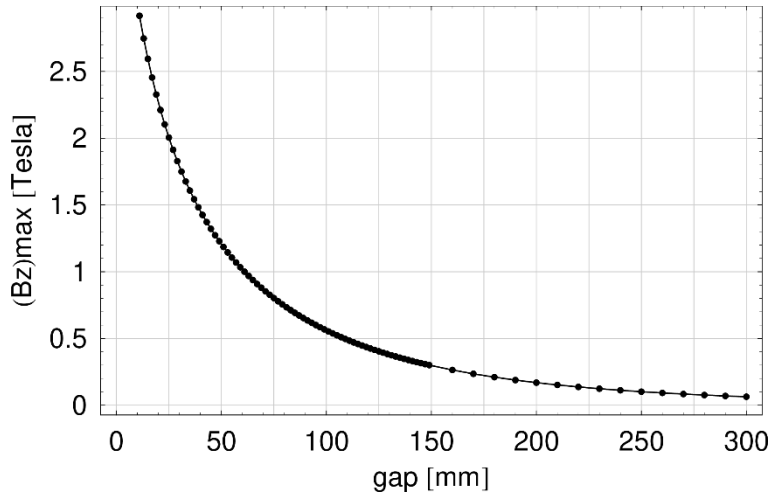

Figure 2: Gap dependence of the peak magnetic field generated at the centre of the 3PW.

The horizontal homogeneity of the magnetic field at the central pole for different gap settings is shown in Figure 3. These plots have been used to determine the field roll-off within different horizontal ranges. The evolution of the roll-off for each considered range as a function of the gap is shown in Figure 4. For the maximum considered horizontal range, +/-20mm, the field roll-off is well within the specified limits (5e-3) for all gaps below 30mm, which is the region of interest for the use of the device as a photon source. For the smaller horizontal ranges, +/-10mm and +/-5mm, the measured roll-off exceeds the specified limits, which is believed to be acceptable (cf. page 13).

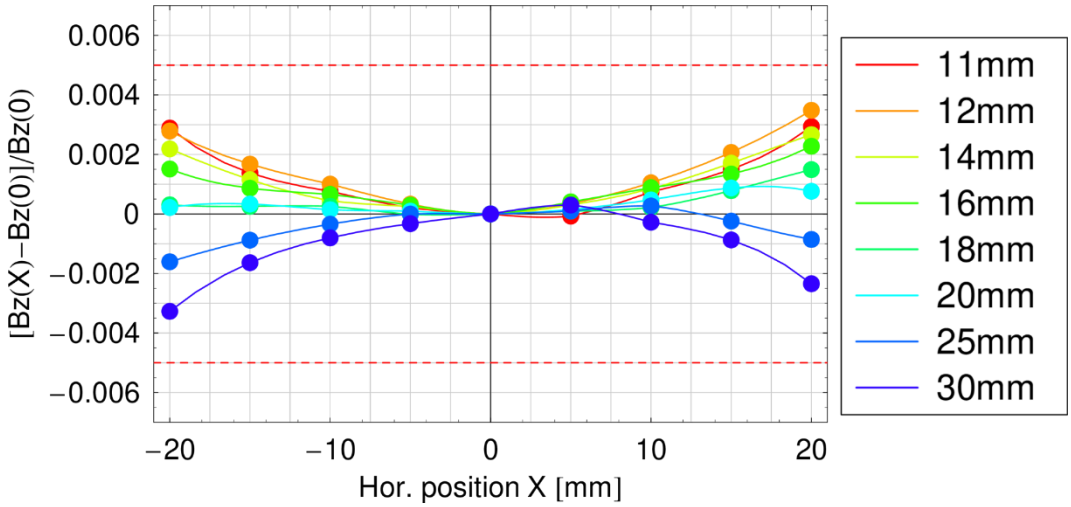

Figure 3: Roll-off of the magnetic field at the central pole for different gap openings. The red dashed lines indicate the limits of the specified value within the range +/-20mm

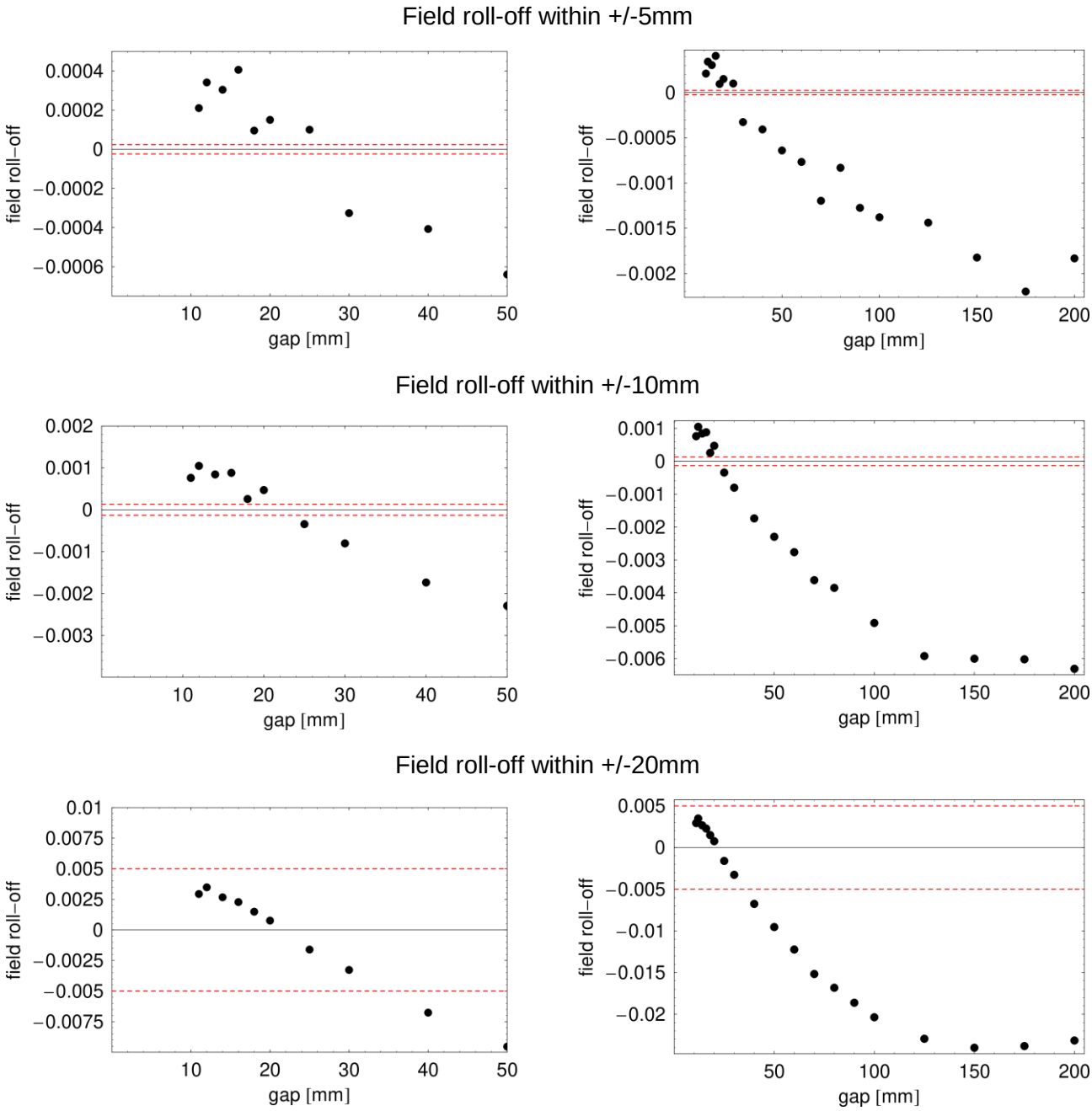

Figure 4: Gap dependence of the field roll-off at the central pole over different horizontal ranges. In each case, the red dashed lines indicate the limits of the specified value (see Table 1).

Integrated measurements: field integrals and multipoles

The gap variation of the on-axis field integrals (first and second) in both planes is shown in Figure 5. Three of the field integral components, namely Ix, I2x and I2z, are within the values specified in Table 1 for the whole range of operational gaps. In the case of Iz, however, the field integral displays a large variation when the gap changes (this had already been anticipated by RADIA simulations). The compromise that has been adopted has been to adjust the value at minimum gap (at gap=11mm a value of $Iz=-9\times10^{-6}$ T·m has been achieved), and the residual values for the other gaps will be actively corrected by means of the correction coils.

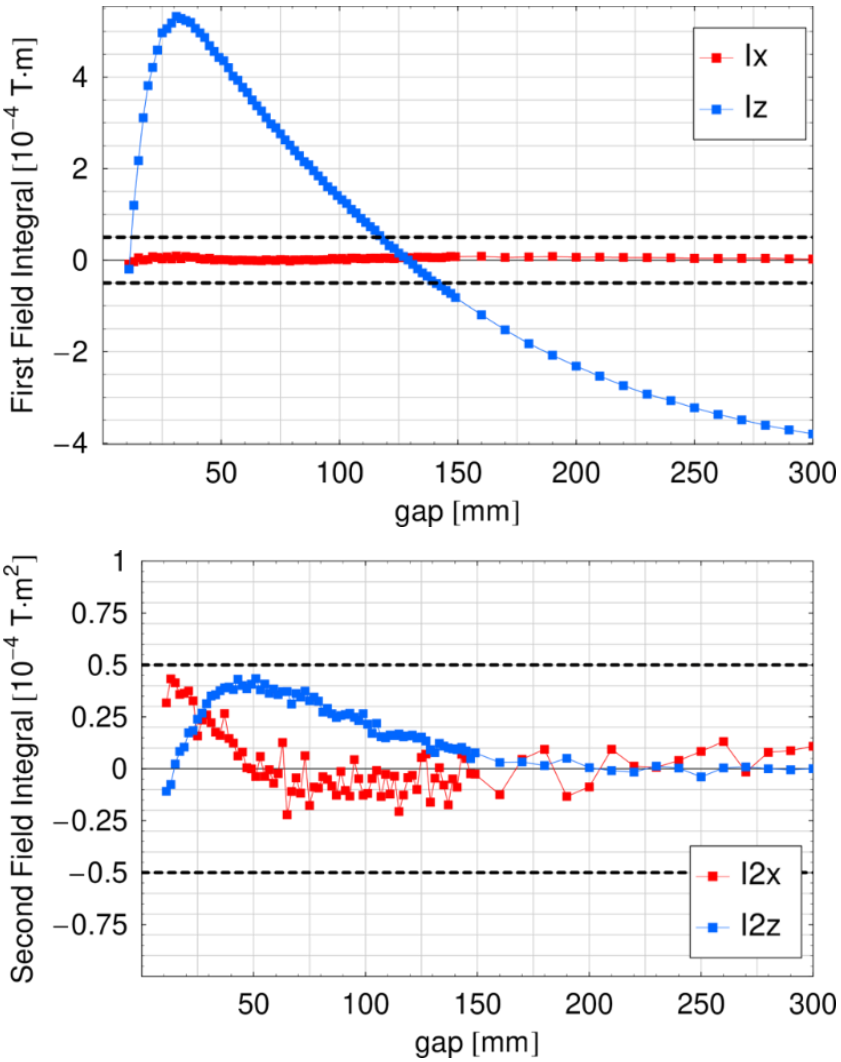

Figure 5: Evolution of on-axis field integrals (top: first field integral; bottom: second field integral) generated by 3PW device as a function of gap. The horizontal dashed lines indicate the specified limit values in each case (see Table 1).

The horizontal dependence of the field integrals has been used to determine the integrated multipoles generated by the device. As an example, Figure 6 shows this dependence determined at minimum gap. In order to obtain the integrated multipoles from this data, a fit of a 6th order polynomial in the range +/-20mm has been carried out, and the multipolar terms have been associated to the different polynomial coefficients (quadrupole → linear term; sextupole → quadratic term; octupole → cubic term; etc).

The resulting gap dependence of the obtained multipoles is shown in Figure 7. In all cases the integrated multipole values are well within the values specified in Table 1.

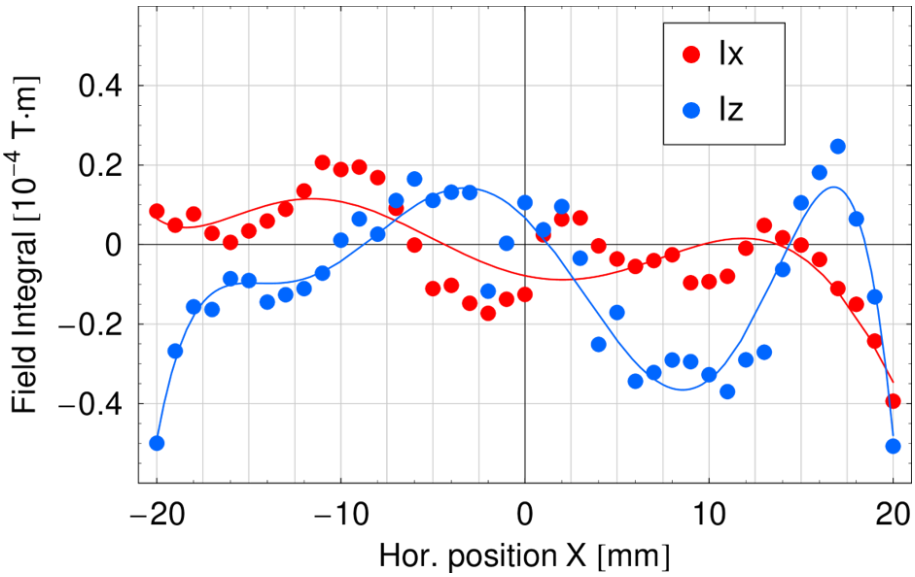

Figure 6: Horizontal dependence of the field integral generated by the 3PW device at minimum gap (=11mm). Solid circles correspond to experimental data determined using the flipping coil, and continuous lines correspond to a 6th order polynomial fit of the experimental data.

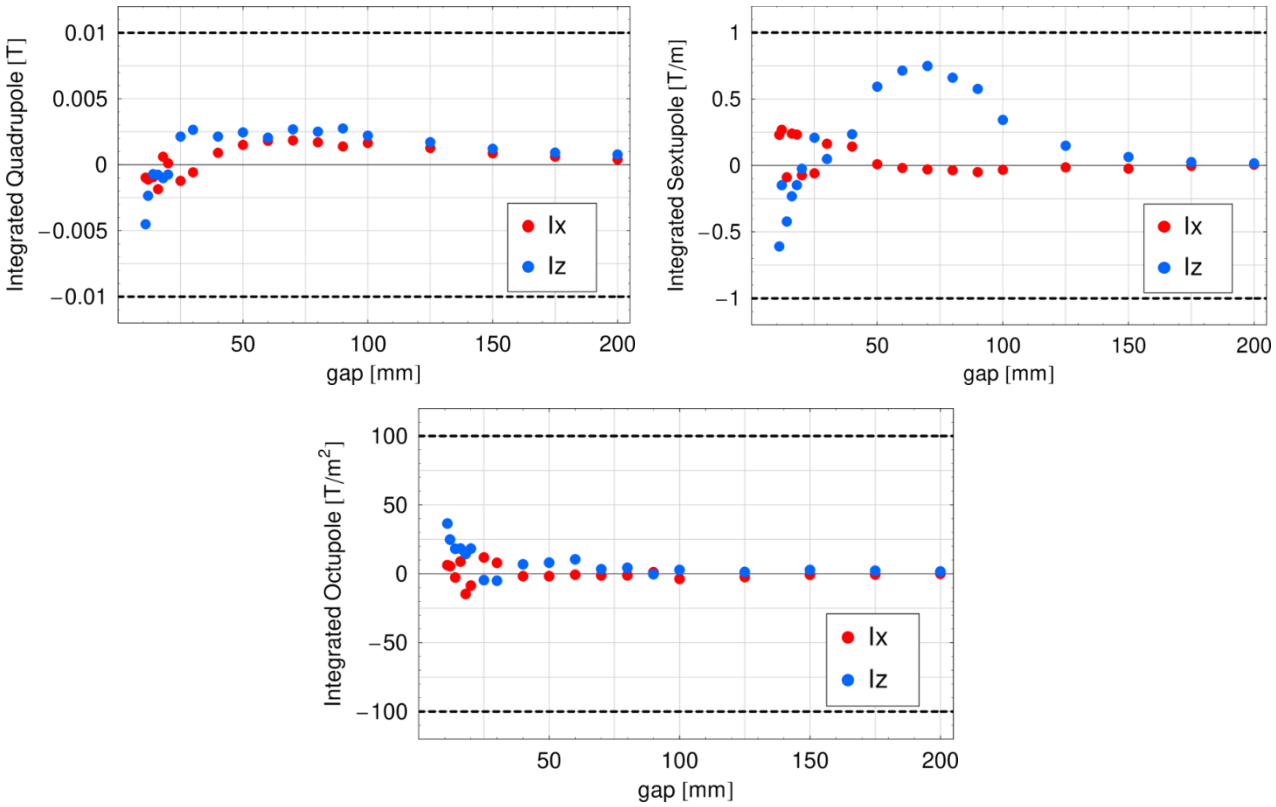

Figure 7: Multipolar terms up to integrated octupole as a function of the gap opening. Blue (red) symbols correspond to normal (skew) multipoles, determined from Iz (Ix) data. The horizontal dashed lines indicate the specified limit values in each case (see Table 1).

Correction coils

In order to correct the residual field integrals shown in Figure 5, the device is equipped with a set of 4 correction coils. As a part of the characterization and acceptance of the device, the field integrals generated by each coil at a given current have been measured. The obtained results are shown in Figure 8, which illustrates that each coil acts on a single plane (either the horizontal or the vertical one). On top of this, due to the fact that the coils are fixed with respect to the insertion device, the effect that they will produce is independent of the gap of the device, as shown in Figure 9.

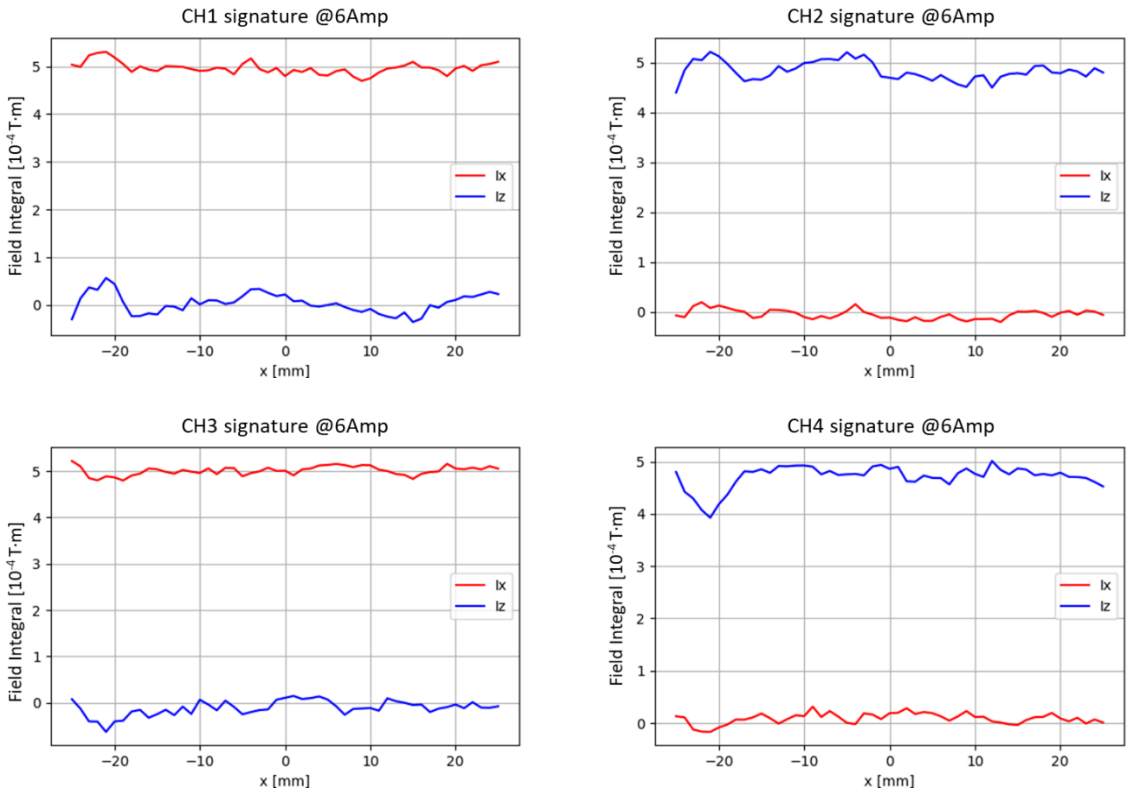

Figure 8: Field integral signatures of each one of the 4 correction coils measured at gap=30mm.

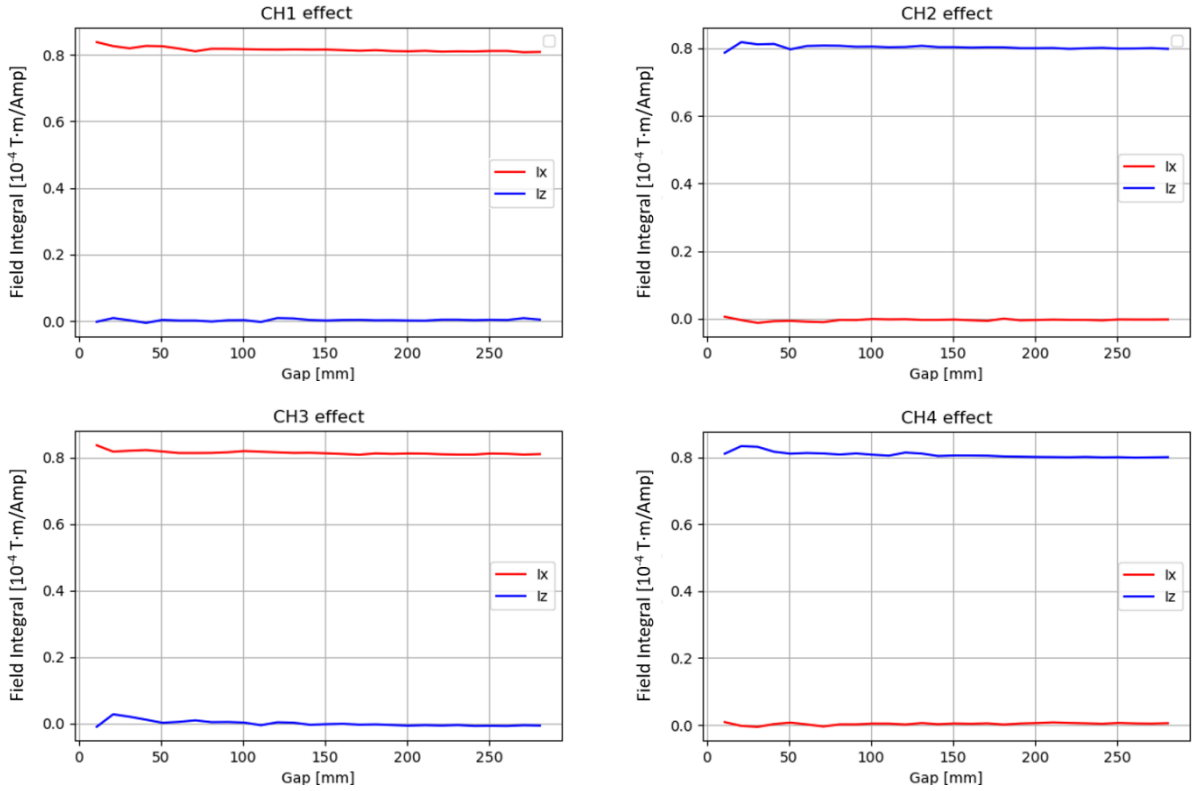

Figure 9: Gap dependence of the on-axis field integrals generated by each one of the correction coils.

From the measurements shown in Figure 8 and Figure 9 we have determined the sensitivity factors of all four coils on the field integrals, as:

	$\frac{dIx}{dI}$ [10^{-5} T m/Amp]	$\frac{dIy}{dI}$ [10^{-5} T m/Amp]	$\frac{dI2x}{dI}$ [10^{-5} T m^2/Amp]	$\frac{dI2y}{dI}$ [10^{-5} T m^2/Amp]
Coil 1	8.27	0	3.00	0
Coil 2	0	8.05	0	2.918
Coil 3	8.35	0	-3.03	0
Coil 4	0	7.96	0	-2.89

Using these sensitivity factors it is possible to determine the currents required to compensate the residual field integrals shown in Figure 5. The obtained values as a function of the gap opening are shown in Figure 10; it can be seen that the maximum required current (~4Amp) is smaller than the operational limit of the coils (10Amp). In order to test the calculated correction, the field integrals generated at 30mm gap have been measured with and without applying the correction, as shown in Figure 11.

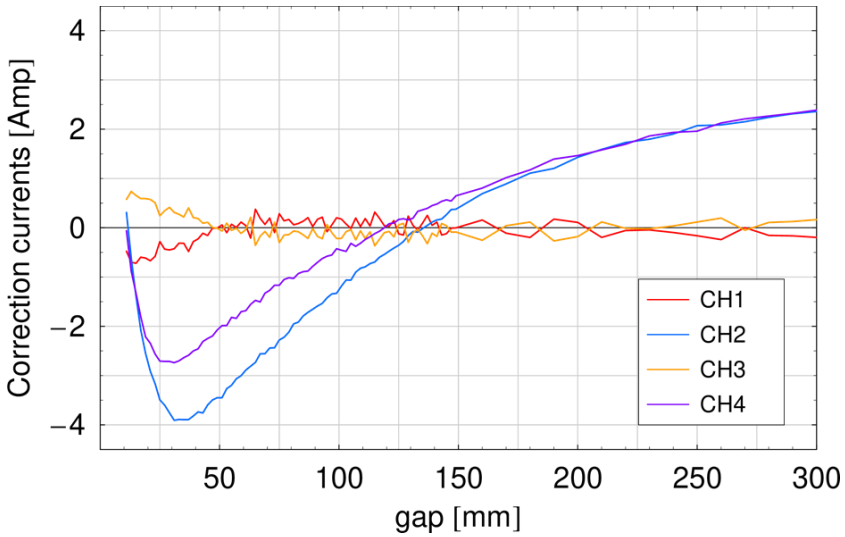

Figure 10: Currents to be applied on the correction coils of 3PW device in order to compensate the residual field integrals generated by the device.

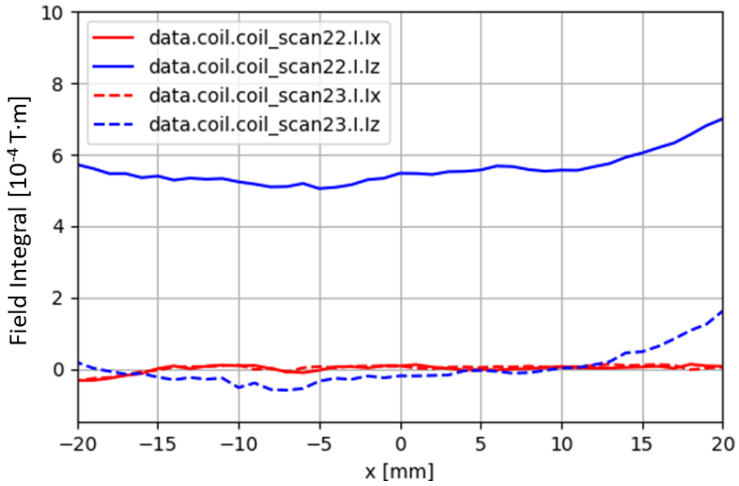

Figure 11: Field integrals generated by the 3PW device at gap=30mm without (solid lines) and with (dashed lines) active correction.

COMPLIANCE WITH SPECIFICATIONS

The compliance of the 3 pole wiggler with the magnetic performance specifications is summarized in Table 2. All requirements are fulfilled unless the field roll-off level within the horizontal ranges +/-5mm and +/-10mm. In a next step, in order to quantify the effect of this deviation on the performance of the SESAME storage ring, the kick map of the device will be calculated using the reported findings and the measured magnetic field map, and fed into a particle tracking code.

Table 2: Compliance of the 3PW device with the magnetic performance specifications.

Parameter	Required value	Compliance	Comments
Peak field of central pole	>2.9 Tesla	✓	0.2917 T @gap=11mm
Field roll off at x=5mm	$<2.4\times10^{-5}$	✗	2×10^{-4}
Field roll off at x=10mm	$<1.3\times10^{-4}$	✗	1×10^{-3}
Field roll off at x=20mm	$<5.0\times10^{-3}$	✓	For gap<30mm
On-axis first field integrals Ix,Iz (no CC)	$<5.0\times10^{-5}$ T·m	✓	Ix only at minimum gap
On-axis second field integrals I2x,I2z (no CC)	$<5.0\times10^{-5}$ T·m^2	✓	Full gap range
Integrated quadrupole within x=±20mm	$<\|1.0\|\times10^{-2}$ T	✓	Full gap range
Integrated sextupole within x=±20mm	<|1.0| T/m	✓	Full gap range
Integrated octupole within x=±20mm	$<\|1.0\|\times10^{2}$ T/m^2	✓	Full gap range